Proceedings of the
47th IEEE Conference on Decision and Control
Cancun, Mexico, Dec. 9-11, 2008

Robust Design of a Spacecraft Attitude Tracking Control System with Actuator Uncertainties

Aranya Chakrabortty[1], Murat Arcak[1] and Panagiotis Tsiotras[2]
[1] Rensselaer Polytechnic Institute, Troy, NY
[2] Georgia Institute of Technology, Atlanta, GA.
Emails: chakra@rpi.edu, arcakm@rpi.edu, tsiotras@gatech.edu

Abstract— **In this paper we apply the robust redesign for transient performance recovery of nonlinear systems with input uncertainties developed in [2] to a spacecraft attitude tracking problem with actuator uncertainties. We first extend the robust design of [2] to a generalized uncertainty structure. Next, we show that when the spin and transverse axis directions and/or the gains of the flywheel actuators are uncertain, the kinematic model of a spacecraft can be expressed in this structure. We apply the extended design to this spacecraft model, illustrate it with a simulation example, and numerically compute the permissible range of the uncertainties for which this design guarantees stability.**

I. INTRODUCTION

Most of the adaptive control designs for attitude tracking problems of spacecraft with parametric model uncertainties are based on the assumption that an exact model of the spacecraft actuator is available [1], [11]. Recent papers such as [13] and [12] have argued that such exact actuator models are rarely available in practice, due to the misalignment of the actuators during installation, aging of the mechanical and electrical components, etc. If the exact directions of the torque axes are not known with sufficient accuracy, then large output torque errors will cause inaccuracy in tracking a reference attitude. Because the control input must compensate for the angular momenta of the flywheels, it is also necessary to know the actuator gains accurately. To address the problems arising from such actuator uncertainties, Yoon and Tsiotras in [13] have proposed a projection-based adaptive control design for a spacecraft whose moment of inertia as well as gimbal axis directions are unknown, and implemented it using Variable Speed Control Moment Gyros (VSCMGs) [8]. However, the closed loop transient responses due to the adaptive design, irrespective of the adaptation gain, can drastically differ from the nominal design, as the parameter estimates are updated dynamically. Since precision in performance is an important factor in spacecraft attitude control, such a loss of nominal performance may be undesirable.

In this paper, we not only achieve reference attitude tracking for the uncertain spacecraft model but also recover the transient trajectories of the nominal model. The approach is to build two sets of high-gain filters - one for estimating the input signal to the plant over a fast time-scale and the other to force this estimate to converge to the nominal input over an intermediate time-scale. Using singular perturbation theory [6], [7], we prove that the trajectories of the redesigned system approach those of the nominal system as the filter gains are increased.

The rest of the paper is organized as follows. In Section 2 we extend the robust design of [2] to a generalized uncertainty structure. In Section 3 we review the nominal dynamic model of a spacecraft and the nominal design as presented in [13]. In Section 4 we characterize the parametric uncertainties in the directions of actuator axes and in the spacecraft inertia matrix, and show that the uncertain model can be expressed in the form studied in Section 2. In Section 5 we apply the robust design of Section 2 to this uncertain model and illustrate the results with a simulation example. We then numerically compute the range of perturbations for which this design guarantees stability. Conclusions are drawn in Section 6.

II. EXTENSION OF THE ROBUST REDESIGN [2] TO A GENERALIZED UNCERTAINTY STRUCTURE

We consider systems of the form

$$\dot{x} \quad = f(x) + g(x)\rho(u,x), \tag{1}$$

where $x \in \mathbb{R}^n$ is the state, $u \in \mathbb{R}^m$ is the control input, $f : \mathbb{R}^n \to \mathbb{R}^n$ and $g : \mathbb{R}^n \to \mathbb{R}^{n\times p}$ are known functions, and $\rho : \mathbb{R}^m \times \mathbb{R}^n \to \mathbb{R}^p$ is an unknown nonlinear function restricted by Assumption 3 below. We assume that all functions are continuously differentiable and $m \geq p$. In [2] and [3] we studied the special case $m = p$ and functions $\rho(u,x)$ of the form $\rho(u,x) = \rho(u)$ and $\rho(u,x) = u + \delta(x)$, respectively, where $\delta(x)$ is an unknown smooth function of the state.

To design a control input u which stabilizes the origin $x = 0$ of (1) despite the unknown $\rho(\cdot,\cdot)$, we first consider the nominal system with $\rho(u,x) = v \in \mathbb{R}^p$ considered as the control input :

Assumption 1: There exists a feedback control law $v = \alpha(x)$ such that the origin of the nominal closed loop system

$$\dot{x} \quad = \quad f(x) + g(x)\alpha(x) \tag{2}$$

is globally asymptotically stable with a positive definite, radially unbounded C^2 Lyapunov function $V_1(x)$ satisfying

$$\frac{\partial V_1}{\partial x}[f(x) + g(x)\alpha(x)] \leq -\beta_1(\|x\|), \quad \forall x \in \mathbb{R}^n, \tag{3}$$

where $\beta_1(\cdot)$ is a class-$\mathcal{K}_\infty$ function, such that $r^2/\beta_1(r)$ is well-defined and continuous for $r > 0$, and there exists a positive constant $\bar{k}$ such that $r^2/\|\beta_1(r)\| \leq \bar{k}$ on any interval of the form $(0, r_0]$, $r_0 > 0$. □

Assumption 2: There exists a function $h : \mathbb{R}^n \to \mathbb{R}^p$ such that the $p \times p$ matrix

$$\gamma(x) := L_g h(x) = \frac{\partial h}{\partial x}\, g(x)$$

is nonsingular for all x. □

Assumption 3: There exists a known C^1 function $S : \mathbb{R}^p \to \mathbb{R}^m$ and a positive number k, independent of x and χ, such that for all $(\chi, x) \in \mathbb{R}^p \times \mathbb{R}^n$,

$$\frac{\partial \rho(S(\chi), x)}{\partial \chi} + \frac{\partial \rho^T(S(\chi), x)}{\partial \chi} \geq k I_{p\times p}, \tag{4}$$

where $I_{p\times p}$ is the $p \times p$ identity matrix . □

When $p = m = 1$ and $\rho(u, x)$ is strictly increasing in u with a uniform lower bound on its slope, Assumption 3 holds with $S(\chi) = \chi$. Likewise, if $\rho(u, x) = \bar{\rho}(x) + Ku$ where $K \in \mathbb{R}^{p\times m}$ is an unknown constant matrix, then Assumption 3 means that a known matrix $S \in \mathbb{R}^{m\times p}$ exists, such that

$$KS + S^T K^T > 0. \tag{5}$$

For example, if K is an uncertain row vector that is known to lie in a cone, then selecting S to be a column vector in the interior of the dual cone guarantees (5). Assumptions similar to (5) are used in MIMO model reference adaptive control as a generalization of the SISO condition that the sign of the high-frequency gain K be known [4], [9].

It follows from [10, Theorem 5.4.5] that Assumption 3 guarantees the existence of the inverse of $\rho(S(\chi), x)$ with respect to χ. Given x, and denoting this inverse function by $\vartheta(\cdot, x) : \mathbb{R}^p \to \mathbb{R}^p$, we note that $\chi = \vartheta(v, x)$ implies

$$\rho(S(\vartheta(v, x)), x) = v. \tag{6}$$

This means that, if $\rho(\cdot, \cdot)$ was perfectly known, then the design

$$u = S(\vartheta(\alpha(x), x)) \tag{7}$$

would lead to the nominal closed-loop system (2). However, since $\rho(\cdot, \cdot)$ is unknown, this design cannot be implemented. We now present a design where we first estimate the signal $v = \rho(u, x)$ by the filtering technique of [2], and then design another feedback loop that forces u to the manifold defined by (7).

With Assumption 2 we note that the variable $y = h(x)$ satisfies

$$\dot{y} \;=\; L_f h(x) + \gamma(x)\rho(u, x). \tag{8}$$

Mimicking (8), we build the filter

$$\dot{\hat{y}} \;=\; L_f h(x) - \frac{\hat{y} - y}{\mu}, \qquad \hat{y}(0) = y(0), \tag{9}$$

where $\mu > 0$. Then the variable

$$\ell := \frac{\hat{y} - y}{\mu} \tag{10}$$

satisfies

$$\mu\,\dot{\ell} \;=\; -\ell - \gamma(x)\rho(u, x), \qquad \ell(0) = 0. \tag{11}$$

When μ is small, ℓ evolves in a faster time-scale than x, and reaches a small neighborhood of the manifold

$$\ell = -\gamma(x)\,\rho(u, x), \tag{12}$$

which means that an estimate for the input signal $v = \rho(u, x)$ is given by $\hat{v} = -\gamma(x)^{-1}\ell$. The following dynamic control law makes use of this estimate and, as we prove in Theorem 1 below, guarantees recovery of nominal system trajectories when the two small parameters $\mu > 0$ and $\epsilon > 0$ are tuned appropriately:

$$\epsilon\,\dot{\chi} \;=\; \alpha(x) + \gamma(x)^{-1}\,\ell, \tag{13}$$

$$u \;=\; S(\alpha(x) + \chi). \tag{14}$$

Since the filter in (13) makes use of the estimate generated by the filter in (11), the speed of convergence of ℓ to a neighborhood of the manifold (12) must be faster compared to the speed of χ; that is, $\mu \ll \epsilon$. Since the two time-scales are dependent on each other, we assign

$$\epsilon = \epsilon_1, \quad \mu = \epsilon_1\epsilon_2 \tag{15}$$

where ϵ_1 and ϵ_2 are now independent small parameters.

The following theorem shows that this redesign recovers the performance of the nominal system and enlarges the region of attraction arbitrarily as $(\epsilon_1, \epsilon_2) \to 0$.

Theorem 1: Given compact sets $\Omega_x \subset \mathbb{R}^n$ and $\Omega_\chi \subset \mathbb{R}^p$, there exists a pair $(\epsilon_1^*, \epsilon_2^*) > 0$ such that for all $0 < \epsilon_1 < \epsilon_1^*$, $0 < \epsilon_2 < \epsilon_2^*$ and for all $x(0) \in \Omega_x$, $\chi(0) \in \Omega_\chi$, the controller (9), (10), (13), (14) guarantees boundedness of $x(t)$, $\chi(t)$ and $\hat{y}(t)$, and convergence of x(t) to the origin. In addition, given any $\xi > 0$, there exist $\epsilon_1^{**} > 0$, $\epsilon_2^{**} > 0$ such that for all $0 < \epsilon_1 < \epsilon_1^{**}$, $0 < \epsilon_2 < \epsilon_2^{**}$, $x(0) \in \Omega_x$ and $\chi(0) \in \Omega_\chi$, the solution $\bar{x}(t)$ of the nominal system (2) and $x(t, \epsilon_1, \epsilon_2)$ of the uncertain system (1) with the redesigned controller (9), (10), (13), (14) satisfy

$$\|x(t, \epsilon_1, \epsilon_2) - \bar{x}(t)\| \leq \xi, \qquad \forall t \geq 0. \tag{16}$$

Proof: The proof follows from the proof of Theorem 1 in [2]. The only difference between the two is in the proof of Lemma 1 which, in this case, follows from Assumption 3.

III. Nominal Dynamic Model for Spacecraft Attitude Motion

We now apply the robust design of Section 2 to recover the nominal closed loop trajectories of the uncertain spacecraft model of [13]. We first describe the nominal dynamic model for the motion of the spacecraft equipped with a VSCMG cluster of N flywheels as discussed in [13]. Figure 1 shows the spacecraft body with the i^{th} VSCMG $(i = 1, \ldots, N)$.

Using the law of conservation of angular momentum, a simplified equation for the spacecraft motion can be written as

$$J\dot{\omega} + C(\gamma_g, \Omega)\dot{\gamma}_g + D(\gamma_g)\dot{\Omega} + \hat{\omega}\bar{h} = 0, \tag{17}$$

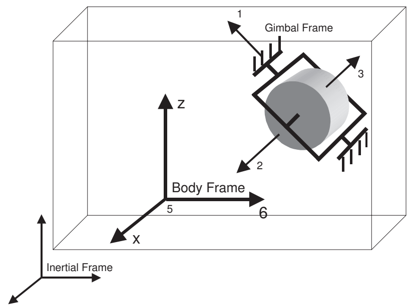

Fig. 1. Spacecraft with a VSCMG configuration.

with

$$\begin{aligned}\bar{h} &:= J\omega + A_s I_{ws}\Omega, &(18)\\ C(\gamma_g,\Omega) &:= A_t I_{ws}\Omega^d, \quad D(\gamma_g) := A_s I_{ws}, &(19)\end{aligned}$$

where $\omega = \text{col}(\omega_1, \omega_2, \omega_3)$ is the angular velocity vector of the spacecraft, $\gamma_g = \text{col}(\gamma_{g1}, ..., \gamma_{gN})$ is the vector of the gimbal angles, $\Omega = \text{col}(\Omega_1, ..., \Omega_N)$ is the vector of wheel speeds of the flywheels with respect to the gimbals, and Ω^d is its diagonal representation. J is the total moment of inertia of the spacecraft given by

$$J = I^B + A_s I_{cs} A_s^T + A_t I_{ct} A_t^T + A_g I_{cg} A_g^T, \quad (20)$$

I_{cg}, I_{cs}, I_{ct} are diagonal matrices of the inertias of the gimbal with flywheel along gimbal axis, spin axis and transverse axis respectively, I_{ws} is a diagonal matrix of the inertia of the flywheel only along the spin axis. A_g, A_s, A_t are $3 \times N$ matrices with columns as the directional unit vectors along the gimbal, spin and transverse axis respectively, I^B is the combined matrix of inertia of the spacecraft platform and the point masses of the VSCMGs, and $\hat{\omega}$ is the skew-symmetric matrix

$$\hat{\omega} = \begin{bmatrix} 0 & -\omega_3 & \omega_2 \\ \omega_3 & 0 & -\omega_1 \\ -\omega_2 & \omega_1 & 0 \end{bmatrix}. \quad (21)$$

The main assumptions in the model (17)-(19) are that the inertia matrix J is constant, the gimbal acceleration is negligible and the angular momentum is independent of the gimbal angular rate. The matrices A_g, A_s and A_t depend on the gimbal angles as

$$\begin{aligned}A_g &= A_{g0}, &(22)\\ A_s &= A_{s0}[\cos\gamma_g]^d + A_{t0}[\sin\gamma_g]^d, &(23)\\ A_t &= A_{t0}[\cos\gamma_g]^d - A_{s0}[\sin\gamma_g]^d, &(24)\end{aligned}$$

where A_{g0}, A_{s0} and A_{t0} are the values of the respective matrices at $\gamma_g = 0$, and $[\cos\gamma_g]^d$, $[\sin\gamma_g]^d$ denote the diagonal representations of $(\cos\gamma_{g1}, ..., \cos\gamma_{gN})$ and $(\sin\gamma_{g1}, ..., \sin\gamma_{gN})$ respectively.

The kinematic equations for the spacecraft are expressed in terms of the modified Rodrigues parameters as

$$\dot{\sigma} = G(\sigma)\omega, \quad (25)$$

where

$$G(\sigma) = 0.5\left(I_{3\times3} + \hat{\sigma} + \sigma\sigma^T - 0.5(1+\sigma^T\sigma)I_{3\times3}\right), \quad (26)$$

and $\hat{\sigma}$ follows the structure in (21). Equations (25) and (17) are combined into one second order equation as

$$\ddot{\sigma} = F^*(\sigma,\dot{\sigma}) + G^*(\sigma,\gamma_g,\Omega)u \quad (27)$$

where,

$$\begin{aligned}F^*(\sigma,\dot{\sigma}) &:= H^{*-1}\Big(G^{-T}JG^{-1}\dot{G}G^{-1}\dot{\sigma}\\ &\qquad -G^{-T}\hat{\omega}R_{\mathcal{I}}^{\mathcal{B}}(\sigma)H_{\mathcal{I}}\Big), &(28)\\ H^*(\sigma) &:= G^{-T}JG^{-1}, &(29)\\ G^*(\sigma,\gamma_g,\Omega) &:= -GJ^{-1}Q, &(30)\\ Q(\gamma_g,\Omega) &:= [C(\gamma_g,\Omega) \;\; D(\gamma_g)], &(31)\end{aligned}$$

$R_{\mathcal{I}}^{\mathcal{B}}(\sigma)$ is the rotation matrix from the inertial frame to the body frame, $H_{\mathcal{I}}$ is the total angular momentum in the body frame, and $u := \text{col}(\dot{\gamma}_g, \dot{\Omega}) \in \mathbb{R}^{2N\times1}$ is the control input vector. Denoting $x_1 = \sigma$, $x_2 = \dot{\sigma}$ and $z := \text{col}(\gamma_g, \Omega) \in \mathbb{R}^{2N\times1}$, the nominal state space model for the spacecraft motion can be written as

$$\begin{aligned}\dot{x}_1 &= x_2, &(32)\\ \dot{x}_2 &= F^*(x_1,x_2) + G^*(x_1,z)u, &(33)\\ \dot{z} &= u. &(34)\end{aligned}$$

Let the reference trajectory to be tracked by the spacecraft be given in terms of the bounded functions σ_d, $\dot{\sigma}_d$, $\ddot{\sigma}_d$ where σ_d denotes the MRP vector for the attitude of a desired frame with respect to the inertial frame. Defining the error variables $e_1 = x_1 - \sigma_d$ and $e_2 = x_2 - \dot{\sigma}_d$, and denoting $e = \text{col}(e_1, e_2)$, we get the error dynamics as

$$\begin{aligned}\dot{e}_1 &= e_2, &(35)\\ \dot{e}_2 &= F^*(e,\sigma_d,\dot{\sigma}_d) + G^*(e,\sigma_d,z)\,u - \ddot{\sigma}_d, &(36)\\ \dot{z} &= u. &(37)\end{aligned}$$

Reference [13] assumes $N \geq 2$ and $G^*(e,\sigma_d,z)$ to be full row rank, and applies the input-output linearization-based nominal design

$$u_{nom} = G^{*\dagger}(e,\sigma_d,z)\underbrace{(\ddot{\sigma}_d - F^*(e,\sigma_d,\dot{\sigma}_d) - Ke)}_{\bar{u}_n(e,\sigma_d,\dot{\sigma}_d,\ddot{\sigma}_d)} \quad (38)$$

for asymptotic tracking of the reference trajectory, where $G^{*\dagger}(e,\sigma_d,z)$ denotes the pseudoinverse of the $3\times2N$ matrix $G^*(e,\sigma_d,z)$, and the 3×6 constant matrix K is chosen such that the eigenvalues of the closed loop system are placed in the desired locations.

IV. Uncertainty Characterization

Following [13], we assume that the exact values of the axis directions at $\gamma_g = 0$ as well as the input scaling gains are unknown, and we have

$$\begin{aligned}A_{s0} &= A_{s0}^n + \Delta A_{s0}, &(39)\\ A_{t0} &= A_{t0}^n + \Delta A_{t0}, &(40)\\ I_{ws} &= I_{ws}^n + \Delta I_{ws}, &(41)\end{aligned}$$

where the superscript n denotes the nominal value of the respective matrices and the prefix Δ denotes an unknown deviation from this nominal value. It can easily be shown that this leads to

$$A_t = A_t^n + \Delta A_t, \quad A_s = A_s^n + \Delta A_s, \qquad (42)$$

where

$$\begin{aligned} A_t^n &= A_{t0}^n[\cos\gamma_g]^d - A_{s0}^n[\sin\gamma_g]^d, && (43)\\ \Delta A_t &= \Delta A_{t0}[\cos\gamma_g]^d - \Delta A_{s0}[\sin\gamma_g]^d, && (44)\\ A_s^n &= A_{s0}^n[\cos\gamma_g]^d + A_{t0}^n[\sin\gamma_g]^d, && (45)\\ \Delta A_s &= \Delta A_{s0}[\cos\gamma_g]^d + \Delta A_{t0}[\sin\gamma_g]^d, && (46)\end{aligned}$$

and hence,

$$C(z) = C^n(z) + \Delta C(z), \quad D(z) = D^n(z) + \Delta D(z),$$

where

$$\begin{aligned} \Delta C(z) &= \left(A_t^n \Delta I_{ws} + \Delta A_t I_{ws}^n + \Delta A_t \Delta I_{ws}\right)\Omega^d, && (47)\\ \Delta D(z) &= \left(A_s^n \Delta I_{ws} + \Delta A_n I_{ws}^n + \Delta A_s \Delta I_{ws}\right). && (48)\end{aligned}$$

When the angular momentum of the VSCMG cluster is unknown due to the uncertainties in the spin axis directions and rotational inertias, we can write

$$\bar{h}(e,\sigma_d,\dot{\sigma}_d,z) = \bar{h}^n(e,\sigma_d,\dot{\sigma}_d,z) + \Delta\bar{h}(z), \qquad (49)$$

where $\Delta\bar{h}(z) = (A_s^n \Delta I_{ws} + \Delta A_s I_{ws}^n + \Delta A_s \Delta I_{ws})\Omega$, and hence,

$$H_{\mathcal{I}}(e,\sigma_d,\dot{\sigma}_d,z) = H_{\mathcal{I}}^n(e,\sigma_d,\dot{\sigma}_d,z) + \Delta H_{\mathcal{I}}(e,\sigma_d,z), \quad (50)$$

where, $\Delta H_{\mathcal{I}}(e,\sigma_d,z) = (R_{\mathcal{I}}^{\mathcal{B}}(e,\sigma_d))^{-1}\Delta\bar{h}(z)$. Thus, following (35)-(36) the uncertain error dynamics can be written as

$$\begin{aligned} \dot{e}_1 &= e_2, && (51)\\ \dot{e}_2 &= F^{*n}(e,\sigma_d,\dot{\sigma}_d) - \ddot{\sigma}_d + \Delta F^*(e,\sigma_d,\dot{\sigma}_d)\\ &\quad + \Big(G^{*n}(e,\sigma_d,z) + \Delta G^*(e,\sigma_d,z)\Big)u, && (52)\\ \dot{z} &= u, && (53)\end{aligned}$$

where,

$$\begin{aligned} F^{*n}(e,\sigma_d,\dot{\sigma}_d) &:= H^{*-1}\Big(G^{-T}JG^{-1}\dot{G}G^{-1}\dot{\sigma}\\ &\qquad -G^{-T}\hat{\omega}R_{\mathcal{I}}^{\mathcal{B}}H_{\mathcal{I}}^n\Big), && (54)\\ \Delta F^*(e,\sigma_d,\dot{\sigma}_d) &= -H^{*-1}\left(G^{-T}\hat{\omega}R_{\mathcal{I}}^{\mathcal{B}}\Delta H_{\mathcal{I}}\right), && (55)\\ G^{*n}(e,\sigma_d,z) &:= -H^{*-1}G^{-T}Q^n, && (56)\\ \Delta G^*(e,\sigma_d,z) &:= -H^{*-1}G^{-T}\Delta Q, && (57)\\ Q^n(z) &:= [C^n(z)\ \ D^n(z)], && (58)\\ \Delta Q(z) &:= [\Delta C(z)\ \ \Delta D(z)]. && (59)\end{aligned}$$

We assume that the gimbals are small enough so that the gimbal motions do not change the inertia matrix J significantly, and, hence, there is no unknown component in J. Next, we apply the redesign of Section 2 to (51)-(59) to recover the closed loop performance of the nominal control system (35)-(38).

V. Nominal Performance Recovery

From equations (35)-(38) we can write the nominal closed loop system as

$$\begin{aligned} \dot{e} &= \bar{K}e, && (60)\\ \dot{z} &= G^{*n\dagger}(e,\sigma_d,z)\,\bar{u}_n(e,\sigma_d,\dot{\sigma}_d,\ddot{\sigma}_d), && (61)\end{aligned}$$

where $\bar{K}$ is Hurwitz by design and, thus, Assumption 1 is satisfied with a quadratic Lyapunov function for the e-subsystem. The nominal control input (38) is

$$u_{nom}(e,t) = G^{*n\dagger}(e,\sigma_d,z(t))\,\bar{u}_n(e,\sigma_d,\dot{\sigma}_d,\ddot{\sigma}_d), \qquad (62)$$

where $z(t)$ is the solution of (61) for $t \geq 0$.

Note that (62) is time-varying whereas the results derived in the proof of Theorem 1 assume the plant (1) as well as the nominal input $\alpha(x)$ to be time-invariant. A perusal of the proof of Theorem 1 shows that the arguments for recovery of trajectories (second part of Theorem 1) do not change in the time-varying case. However, convergence of the error e to the origin (first part of Theorem 1) must be replaced by convergence to an $\mathcal{O}(\epsilon_1\epsilon_2)$ residual set around $e = 0$. Likewise, a stability analysis for the z-subsystem is not pursued here. We assume that the reference signal σ_d is such that z remains bounded.

Assumption 2 is satisfied by considering the relative-degree one output as e_2. To satisfy Assumption 3 we write (51)-(52) as

$$\begin{aligned} \dot{e}_1 &= e_2,\\ \dot{e}_2 &= f_n(e,\sigma_d,\dot{\sigma}_d,\ddot{\sigma}_d) + \rho_1(e,\sigma_d,\dot{\sigma}_d,z) + \rho_2(e,\sigma_d,z)u,\end{aligned}$$

where

$$f_n(e,\sigma_d,\dot{\sigma}_d,\ddot{\sigma}_d) = F^{*n}(e,\sigma_d,\dot{\sigma}_d) - \ddot{\sigma}_d \qquad (63)$$

is known, and the functions

$$\rho_1(e,\sigma_d,\dot{\sigma}_d) = \Delta F^*(e,\sigma_d,\dot{\sigma}_d) \qquad (64)$$

and

$$\rho_2(e_1,\sigma_d,z) = G^{*n}(e,\sigma_d,z) + \Delta G^*(e,\sigma_d,z) \qquad (65)$$

are unknown. Since by our time-scale separation design in Section 2 we want to drive the estimate of

$$\rho = \rho_1(e,\sigma_d,\dot{\sigma}_d,z) + \rho_2(e,\sigma_d,z)\,u \qquad (66)$$

to $G^{*n}(e,\sigma_d,z)\,u_{nom}$ as designed in (38), we define the function S, required by Assumption 3, as:

$$S(\chi) = G^{*n\dagger}(e,\sigma_d,z)\chi \qquad (67)$$

where the $2N \times 3$ matrix $G^{*n\dagger}(e,\sigma_d,z)$ is the pseudoinverse of $G^{*n}(e,\sigma_d,z)$. Therefore, from (65) and (67), condition (4) becomes :

$$(G^{*n} + \Delta G^*)\,G^{*n\dagger} + (G^{*n\dagger})^T\,(G^{*n} + \Delta G^*)^T \geq k\,I_{3\times 3}$$

or equivalently,

$$P(e,\sigma_d,z) + P(e,\sigma_d,z)^T \geq k\,I_{3\times 3}, \qquad (68)$$

for all time $t \geq 0$, where

$$P(e, \sigma_d, z) = \underbrace{GJ^{-1}(Q^n + \Delta Q)}_{3\times 2N}\underbrace{(GJ^{-1}Q^n)^{\dagger}}_{2N\times 3}. \quad (69)$$

The expression for $P(e, \sigma_d, z)$ in (69) follows from (30). As $\Delta Q \to 0$ in (69), $P(e_1, \sigma_d, z) \to I_{3\times 3}$, and (68) is satisfied with $k = 1$. Therefore, it is fair to assume that (68) holds for small ΔQ. In Section 6 we numerically investigate the extent of this perturbation under which (68) holds.

To recover nominal performance we build the filter

$$\dot{\hat{e}}_2 = f_n(e, \sigma_d, \dot{\sigma}_d, \ddot{\sigma}_d) - \frac{\hat{e}_2 - e_2}{\epsilon_1 \epsilon_2}, \qquad \hat{e}_2(0) = e_2(0),$$

and define the variable $\ell = (\hat{e}_2 - e_2)/\epsilon_1\epsilon_2$ so that ℓ satisfies

$$\epsilon_1\epsilon_2\dot{\ell} = -\ell - \rho_1(e, \sigma_d, \dot{\sigma}_d) - \rho_2(e, \sigma_d, z)u, \qquad \ell(0) = 0.$$

We then build the second filter

$$\epsilon_2\, \dot{\chi} = -f_n(e, \sigma_d, \dot{\sigma}_d, \ddot{\sigma}_d) - Ke + \ell,$$

and redesign the control input as

$$u = u_{nom} + G^{*n\dagger}(e, \sigma_d, z)\, \chi, \quad (70)$$

where K and u_{nom} follow from (38).

VI. Simulation Results

In this section we present a numerical example of a satellite with a VSCMG cluster with four flywheels (i.e., $N = 4$), to show the effectiveness of the time-scale separation design discussed in Section 2. As in [13] we assume a standard four-VSCMG pyramid configuration with the simulation parameters shown in Table 1.

We assume that the nominal axis directions at $\gamma_g = 0$ are given by

$$A^n_{s0} = \begin{bmatrix} 0 & -1 & 0 & 1 \\ 1 & 0 & -1 & 0 \\ 0 & 0 & 0 & 0 \end{bmatrix}, \quad (71)$$

$$A^n_{t0} = \begin{bmatrix} -0.5774 & 0 & 0.5774 & 0 \\ 0 & -0.5774 & 0 & 0.5774 \\ 0.8165 & 0.8165 & 0.8165 & 0.8165 \end{bmatrix} \quad (72)$$

while the actual axis directions at $\gamma_g = 0$ are

$$A_{s0} = \begin{bmatrix} 0.0192 & -0.9984 & -0.0396 & 0.9984 \\ 0.9990 & -0.0404 & -0.9990 & -0.0396 \\ -0.0404 & -0.0396 & -0.0208 & -0.0404 \end{bmatrix}, \quad (73)$$

$$A_{t0} = \begin{bmatrix} -0.5438 & -0.0101 & 0.5435 & 0.0556 \\ 0.0443 & -0.5611 & -0.0390 & 0.5598 \\ 0.8380 & 0.8277 & 0.8385 & 0.8268 \end{bmatrix} \quad (74)$$

which are obtained by slightly perturbing the nominal axis directions. Hence, the uncertainties in these matrices are characterized by

$$\Delta A_{s0} = A_{s0} - A^n_{s0}, \quad \Delta A_{t0} = A_{t0} - A^n_{t0}. \quad (75)$$

In addition, the nominal and the actual values of the moments of inertia of the flywheels along their spin axis are respectively assumed to be

$$I^n_{ws} = [2.0, 2.0, 2.0, 2.0]^d \quad \mathrm{kg\, m}^2 \quad (76)$$

$$I_{ws} = [1.98, 2.01, 2.02, 1.99]^d \quad \mathrm{kg\, m}^2 \quad (77)$$

where the superscript d denotes the diagonal representation of the respective vectors. The actual value of $H_{\mathcal{I}}$ is given by

$$H_{\mathcal{I}} = [-194.6, -628.2, -885.9] \quad \mathrm{kg\, m}^2/\mathrm{sec}. \quad (78)$$

The matrix K in (38) is chosen such that the closed loop linear e-subsystem has eigenvalues

$$\lambda \in \left\{-0.2\sqrt{2}, -0.2\sqrt{2}, -0.2\sqrt{2}, -0.3\sqrt{2}, -0.3\sqrt{2}, -0.3\sqrt{2}\right\}.$$

The reference trajectory is chosen so that the initial reference attitude is aligned with the inertial frame, and the angular velocity of the reference attitude is chosen as

$$\omega_d(t) := \dot{\sigma}_d = (0.04\sin(2\pi t/400),\, 0.04\sin(2\pi t/300),\, 0.04\sin(2\pi t/200))^T \ \mathrm{rad/sec}. \quad (79)$$

The nominal design as well as the redesign are simulated using Matlab. Figures 2(a), 2(b) show the tracking of the first two components of the reference attitude $\sigma_d(t)$ by the nominal design (38). Figure 3 shows how the error $e_1 :=$

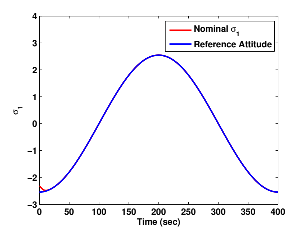

(a) Nominal response of σ_1

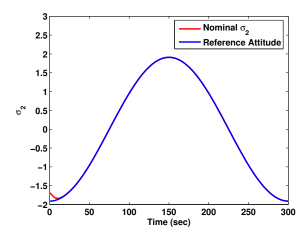

(b) Nominal response of σ_2

Fig. 2. Nominal tracking of σ_d

$\sigma_1 - \sigma_{d1}$ for the uncertain system (51)-(59) approaches the nominal error response when the three-time scale design is applied and the filter gains are gradually increased. Similar figures can be drawn for the other two components of the attitude. Figures 4(a)-4(b) show the close matching between the nominal tracking of the first two components of the reference velocity $\omega_d(t)$ and the redesigned tracking with $\epsilon_1 = \epsilon_2 = 0.1$. Even finer matching can be obtained by using smaller values of (ϵ_1, ϵ_2). Figures 5(a) and 5(b) show the responses of the first and fifth component of the control input vector for the redesigned system vs the nominal system, for the first 20 seconds.

To investigate the extent of perturbations in the spin and transverse axis directions for which the design is feasible for this example, we multiply the direction matrices in (73) and (74) by a constant number b while keeping the nominal axes fixed, and compute the maximum value of b for each matrix separately such that (68) holds. This is done algebraically by setting up a numerical grid consisting of $\sigma_{d_i} \in [-4, 4]$ in steps of 0.5 for $i = 1, 2, 3$, $\sigma_i \in [-3, 3]$ in steps of 0.5

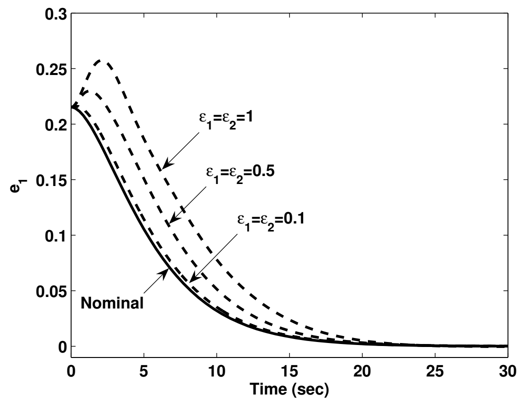

Fig. 3. Recovery of the nominal error response $e_1 = (\sigma_1 - \sigma_{1d})$ by decreasing ϵ_1 and ϵ_2

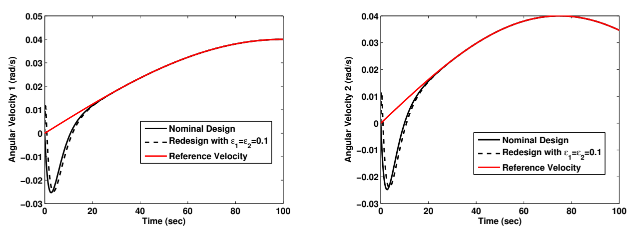

(a) Recovery of $\dot{\sigma}_1$ (b) Recovery of $\dot{\sigma}_2$

Fig. 4. Recovery of the nominal velocity-tracking by using a small filter gain ($\epsilon_1 = \epsilon_2 = 0.1$)

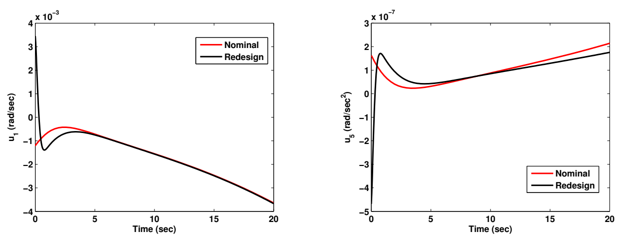

(a) u_1 (b) u_5

Fig. 5. Comparison of nominal and redesigned control inputs for ($\epsilon_1 = \epsilon_2 = 0.1$)

for $i = 1, 2, 3$, $\gamma_{gi} \in [-0.2, 0.2]$ rad in steps of 0.1 rad for $i = 1, 2, 3, 4$, and numerically computing the eigenvalues of the symmetric part of $P(e, \sigma_d, z)$ over each point in this grid. For computational simplicity it is assumed that changes in Ω is negligible compared to its initial high value. Computations show that the eigenvalues of P are more sensitive to the perturbations in A_{t0} than A_{s0}. When the reference attitude is given by (79) then $b = 1.205$ for A_{s0}, and $b = 1.02$ for A_{t0}. These numbers, however, represent more than 20.5% and 2% perturbations in the respective nominal matrices since the actual perturbation is given as

$$\begin{aligned} \Delta\bar{A}_{*0} &= (A^n_{*0} + \Delta A_{*0})b - A^n_{*0} && (80) \\ &= (b-1)A^n_{*0} + b\,\Delta A_{*0} && (81) \end{aligned}$$

where $\Delta A_{*0} = A_{*0} - A^n_{*0}$ are the perturbations considered in the respective matrices in (71)- (74), and $* = s, t$.

VII. Conclusion

In this paper we applied a time-scale separation redesign for nominal performance recovery of a spacecraft attitude control problem when the exact directions of the spin and transverse axes, the gains of the flywheel actuators and the inertia matrix are unknown. As is typical to any high-gain design, one demerit of this method is that the control input might peak in transience, which comes as a trade-off between the affordable control effort and the closeness of trajectories.

TABLE I

Simulation Parameter

Symbols	Parameter Values	Units
N	4	-
$\omega(0)$	$[0,0,0]^T$	rad/sec
$\dot{\omega}(0)$	$[0,0,0]^T$	rad/sec^2
$e(0)$	$[0.2153, 0.2153, 0.2153]^T$	-
$\gamma(0)$	$[0,0,0,0]^T$	rad
$\Omega(0)$	$3.0 \times 10^4[1,1,1,1]^T$	rpm
I^B	$\begin{bmatrix} 15000 & 3000 & -1000 \\ 3000 & 6500 & 2000 \\ -1000 & 2000 & 12000 \end{bmatrix}$	kg m^2
I_{cg}	$(0.7, 0.7, 0.7, 0.7)^d$	kg m^2
I_{wt}, I_{wg}	$(0.4, 0.4, 0.4, 0.4)^d$	kg m^2
I_{gs}, I_{gt}, I_{gg}	$(0.1, 0.1, 0.1, 0.1)^d$	kg m^2

References

[1] J. Ahmed, V. Coppola, and D. Bernstein, "Adaptive Asymptotic Tracking of Spacecraft Attitude Motion with Inertia Matrix Identification," *Journal of Guidance, Control, and Dynamics*, vol. 21, no. 5, 1998, pp. 684-691.

[2] A. Chakrabortty and M. Arcak, "A Three Time-scale Redesign for Stabilization and Performance Recovery of Nonlinear Systems with Input Uncertainties," *in Proceedings of the* 46^{th} *Conference on Decision and Control,* New Orleans, LA, pp. 3484-3489, 2007.

[3] A. Chakrabortty and M. Arcak, *in Proceedings of the American Control Conference,* New York, NY, pp.4643-4648, 2007.

[4] P. Ioannou and J. Sun, *Robust Adaptive Control*, Prentice Hall, NJ, 1996.

[5] A. Isidori, *Nonlinear Control Systems*, 3^{rd} edition, Springer-Verlag, London, 1995.

[6] H. K. Khalil, *Nonlinear Systems*, Prentice Hall, NJ, 2002.

[7] P. Kokotovic, H. Khalil, and J. O' Reilly, *Singular Perturbation Methods in Control: Analysis and Design*, Academic Press, 1986.

[8] H. Kurokawa, *A Geometric Study of Single Gimbal Control Moment Gyros - Singularity Problems and Steering Law*, ME Lab report no. 175, p.108, Agency of Industrial Technology & Science, Ministry of International Trade and Industry, Japan, 1998.

[9] K. S. Narendra and A. M. Annaswamy, *Stable Adaptive Control*, Prentice Hall, NJ, 1989.

[10] J. M. Ortega and W. C. Rheinboldt, "Iterative Solutions of Nonlinear Equations in Several Variables," *SIAM Classics in Applied Mathematics*, Philadelphia, 2000.

[11] J. J. E. Slotine, and M. D. D. Benedetto, *IEEE Transactions on Automatic Control*, vol. 35, July 1990, pp. 848-852.

[12] H. Yoon and P. Tsiotras, "Spacecraft Adaptive Attitude and Power Tracking with Variable Speed Control Moment Gyroscopes," *Journal of Guidance, Control, and Dynamics*, vol. 25, 2002, pp. 1081-1090.

[13] H. Yoon and P. Tsiotras, "Adaptive Spacecraft Attitude Tracking Control with Actuator Uncertainties," *in Proceedings of the AIAA Guidance, Navigation, and Control Conference*, AIAA Paper 05-6392, San Francisco, CA, 2005.